

Validation of Aura MLS OH Measurement with FTUVS Total OH Column Measurement at TMF, California

Shuhui Wang¹, Herbert M. Pickett¹, Thomas J. Pongetti¹, Ross Cheung², Yuk L. Yung²,
Changsub Shim¹, Qinbin Li¹, Timothy Canty³, Ross J. Salawitch³ and Stanley P. Sander¹

(Tentative author list)

¹ Jet Propulsion Laboratory, California Institute of Technology, Pasadena, CA

² Division of Geological and Planetary Sciences, California Institute of Technology,
Pasadena, CA

³ Department of Atmospheric & Oceanic Science / Department of Chemistry &
Biochemistry, University of Maryland, College Park

Abstract

The first seasonal and interannual validation of OH measurements by Microwave Limb Sounder (MLS) onboard Aura has been conducted with ground-based OH column abundance measurements by Fourier Transform Ultra-Violet Spectrometer (FTUVS) over JPL's Table Mountain Facility (TMF) during 2004 – 2007.

The MLS OH densities over TMF area are integrated vertically at altitudes with pressure of 21.5 hPa and below to get a partial OH column for a comparison with TMF OH column data. The missing OH residual in the lower stratosphere and the troposphere is determined by GEOS-Chem monthly mean OH outputs and the diurnal variation of OH from observations and photochemical model calculations. Further model calculations with hourly OH outputs during selected months justify this approach. In addition, a number of field observations from air-borne instruments as well as calculations from JPL 1-D photochemical HO_x model are compared to the GEOS-Chem results to estimate the uncertainty in the OH residual.

In general, the combined total OH columns from MLS and GEOS-Chem agree with TMF total OH column, especially during seasons with high OH. In winter with low OH, the former is often higher than the latter. At solar zenith angles (SZAs) above 50°, the mean of the former is 10.5% larger than the latter. Various statistical approaches are applied to investigate the correlation of these results. A standard linear fit through origin shows a remarkable agreement within 6.5%, while an orthogonal linear fit with error bars of both measurements weighted gives a slope of 0.835 and an intercept of $1.308 \times 10^{13} \text{ cm}^{-2}$, which implies a weaker seasonal variation in MLS measurements than TMF measurements and a possible offset between them. Seasonal and SZA variation studies confirm this trend. Further investigations with more complete datasets are required to fully understand the observed differences.

1. Introduction

Ozone in the stratosphere and the lower mesosphere plays an important role in affecting global stratosphere temperature and circulation [Muller et al., 1999]. While halogen species are mainly responsible for the ozone loss trend at about 40 km, above this altitude and below 22 km, the major catalytic ozone loss is controlled by reactions involving odd hydrogen species HO_x[Osterman, et al., 2005][Salawitch, et al., 2005]. Since OH is a key species in many of these reactions, it is essential to obtain systematic and long term measurements of OH.

The NASA Aura satellite was launched on July 15th, 2004 into a sun-synchronous orbit. The Earth Observing System Microwave Limb Sounder (EOS MLS) onboard Aura has been providing measurements of a number of chemical species including OH for over three years [Waters et al, 2006]. Early validation of MLS measurements for several molecules was reported by [Froidevaux et al, 2006]. The validation of OH measurements was conducted for a short period in September, 2004 with Balloon OH instrument (BOH) and Far Infrared Spectrometer (FIRS-2) launched from Ft. Sumner, NM [Pickett et al, 2006]. It was found that the OH columns above 40 km from these measurements agree within 8%, while the OH densities at 25 – 40 km altitudes agree within 17% among these measurements. The version 1.51 retrieval software was used. More recently, MLS HO_x products from version 2.2 software, which has a substantial improvement from v1.51 for mesospheric OH and stratospheric HO₂, were validated for September 23rd, 2004 and September 20th, 2005 [Pickett et al, 2007]. The updated MLS OH results agree with the BOH and FIRS-2 measurements within 15% in 2004 and 18% in 2005, respectively. Results from a 1-D photochemical model constrained with OH precursors measured by MLS also agree with MLS OH profiles within MLS measurement precision. OH column abundance measurements from Poly-etalon Pressure Scanned Interferometric Optical Spectrometer (PEPSIOS) and FTUVS were also compared with the MLS measurements. The validation for the other time of the year, however, has not been reported so far.

The Jet Propulsion Laboratory's Fourier Transform Ultra-Violet Spectrometer (FTUVS) has been providing reliable ground-based total OH column measurements at Table Mountain Facility (TMF) in southern California (34.4°N, 117.7°W) for a decade [Cageao et al, 2001][Mills et al, 2002, 2003][Li et al, 2005]. There are sufficient overlapping days with both MLS and TMF OH measurements during 2004 – 2007, which offers an excellent opportunity to validate the seasonal and inter-annual variation of MLS OH data by comparing the OH columns from both measurements. Since the MLS OH density measurements have useful precision above about 25 km, the OH column data from MLS measurements cover near 90% of the total OH abundance in the atmosphere. The missing OH residual in the lower stratosphere and the troposphere has to be estimated in order for a comparison of the total OH columns from MLS and TMF. In the present work, this missing partial OH column is estimated based on OH profiles modeled by GEOS-Chem. It is also compared with other observations and calculations from a 1-D HO_x photochemical model [Canty et al., 2006]. The estimated OH residual is combined with the MLS OH data to get a total OH column at latitudes and longitudes similar to TMF, which is then compared to the TMF OH column data at the Aura satellite overpass time. The overall agreement and the agreement at different seasons and different SZAs are presented. Possible causes of differences are discussed.

2. Experimental techniques and model description

2.1 Microwave Limb Sounder (MLS) on Aura

The MLS instrument contains heterodyne radiometers that observe the thermal emissions from the atmospheric limb in five spectral regions continuously during day and night. OH is measured at 2.5 THz in stratosphere and mesosphere. The daytime measurements are corrected by the nighttime measurements to eliminate the instrument offset. (*Herb might want to add more details here*) Detailed description of the OH measurement technique and the instrument calibration is given by [Pickett, 2006].

The OH products used in this study is from v2.2 retrieval software unless otherwise specified. The difference between v2.2 and the previous version v1.51 for OH are

discussed in [Pickett et al, 2007]. For validation purpose, MLS OH data at a latitude range of [29.5°N, 39.5°N] and a longitude range of [130.15°W, 105.15°W] were extracted for selected days. Due to their poor precision in the lower atmosphere, OH densities below 21.5 hPa were not considered. The extracted OH data was integrated vertically to get partial OH columns from 21.5 hPa to the upper mesosphere.

The Aura satellite is in a sun-synchronous orbit. The time when the MLS field of view scans the latitudes and longitudes covering TMF is often between 21:00 – 21:30 UT with a small variation from day to day. To be accurate, the altitude-corrected SZA is used as the primary criterion to match the TMF data points with the MLS measurements for any given day.

2.2 High-resolution Fourier Transform Ultra-Violet Spectrometer (FTUVS) at TMF

High resolution FTUVS has been used to measure the total OH column abundance over TMF since July 1997. Reliable data are obtained during days with clear to partially cloudy conditions. [Cageao et al, 2001] provided a detailed description of the instrument system and the data retrieval process. The objective OH absorption lines fall in the region of strong solar Fraunhofer lines. The FTUVS telescope views the Sun's east and west limbs alternatively and the Doppler shift between these spectra due to solar rotation is used to separate terrestrial OH lines from the strong solar lines. During one measurement cycle (~15 minutes for each limb), the Doppler shift magnitude is approximately 0.28 cm^{-1} . The west limb spectra are shifted to match the east limb spectra. By dividing the east spectra with the shifted west spectra, ideally, the solar Fraunhofer features should be removed, leaving the terrestrial OH lines. Given a modeled Doppler broadened OH line shape, the corresponding absorption cross section, and the measured air mass factor, the OH column abundance is retrieved from the spectral fit.

The primary source of uncertainty in the measured OH column is the spectral fit [Cageao et al, 2001] [Li et al, 2005]. A number of improvements to the spectral analysis program were made very recently, leading to a significant decrease in the spectral fit uncertainties [Cheung et al, 2007].

For the first time, a Fast Fourier Transform (FFT) smoothing technique is adopted to describe the remaining broad-band solar background feature in the East/West ratio

spectra. This allows for a further correction of the background curvature prior to the OH line fit. A conjugate-gradient fit, which is more efficient than the traditional shift-and-scale fit, is employed over a much narrower spectral window (nano-window) selected empirically. The FFT correction of the solar baseline combined with the conjugate-gradient fit results in a reduction of the spectral fit variance by up to 60% [Cheung et al, 2007]. In particular, the spectral fit quality of several weak OH lines has been greatly improved so that a more reliable multiple-absorption-line analysis can be used to further improve the precision. Traditionally, only P₁(1) line (32440.57cm⁻¹) is analyzed because of its line strength and the least influence from the solar baseline curvature. [Mills et al, 2002, 2003] adopted Q₁(2) as an additional line and showed an acceptable agreement between Q₁(2) and P₁(1) results. [Li et al, 2005] further expanded the analysis to five OH lines and used the diurnal variability as a weighting factor to average the results. Different from the previous multi-line analysis techniques, the current retrieval introduces an advanced “dynamic line selection”, which accepts OH lines that reduce the deviation of the weighted average from a 2nd order polynomial fit of the diurnal variation but rejects lines that merely contribute more random noise. The weighted average is based on the signal-to-noise ratio (SNR) of each selected absorption line. SNR is empirically proved to be more reliable than the previously adopted weighting factors since it takes both the quality of the signal and the quality of the spectral fit into account without making assumptions of the diurnal variation pattern. This improved multi-line retrieval method leads to a significant reduction in the scatter of the results [Cheung et al, 2007].

Since MLS overpass time is close to the local noon, OH line signals around overpass time are generally strong and of good quality. During most clear summer days, five OH lines are averaged, while only three strongest lines are dynamically selected during a typical winter day. In several extreme cases with particularly weak OH signals even around noon time, only P₁(1) and Q₁(2) contribute to the weighted average.

2.3 GEOS-Chem model description

GEOS-Chem is a global 3-D chemical transport model driven by assimilated meteorological data from NASA Global Modeling Assimilation Office (GMAO). A comprehensive tropospheric O₃-NO_x-VOC chemistry mechanism is included. Detailed

model description and evaluation are given in [Bey et al., 2001]. GEOS-Chem has been extensively validated and used to study a variety of atmospheric phenomena. It is proved to be a useful tool for studying the global tropospheric distribution of OH [Bloss et al., 2005].

In the present work, the versions v5-07-08 and v7-04-10 are used (see http://www.as.harvard.edu/chemistry/trop/geos/geos_versions.html for version history). The major differences between these versions are listed in Table 1. The 3-D meteorological fields are updated every six hours. The surface fields and mixing depths are updated every three hours. Climatological monthly mean biomass burning emissions are from [Duncan et al., 2003]. The emission inventory of v5-07-08 is from the Global Emission Inventory Activity (GEIA). In v7-04-10, the fossil fuel emissions for NO_x, CO, and SO₂ are from the Emission Database for Global Atmospheric Research (EDGAR), while the emission inventory for the other species are from GEIA. [Benkovitz et al., 1996][Olivier et al., 2001].

The 2°×2.5° model grid covering TMF has a latitude range of [33.0°N, 35.0°N] and a longitude range of [117.5°W, 120.0°W], a significant part of which is over the Pacific ocean. The average elevation in the model grid is thus lower than the elevation of TMF (~2.25 km). This difference is taken into account in the calculation of OH columns over TMF.

3. Results

3.1 MLS partial OH column and TMF total OH column

The MLS v2.2 partial OH columns above 21.5 hPa over TMF area on selected days are plotted in Figure 1. For a close comparison, the selection only includes days when TMF measurements are available on the same day or one day away. The altitude-corrected SZA of MLS measurements are plotted in the lower panel of Figure 1. The corresponding time at TMF area was calculated with Multiyear Interactive Computer Almanac (MICA) from U.S. Naval Observatory. In most cases, the calculated “overpass time” is between

21:00 – 21:30 UT with a mean of 21:06 UT. Since the overpass time has a small variation from day to day, it is more accurate to use SZA as the criterion to select TMF data points for a comparison with MLS data.

The FTUVS instrument measures OH by looking at the east and west limbs of the sun alternatively and then taking the ratio of east/west limbs to remove the strong solar lines in the spectra. A typical measurement cycle takes about 30 min, during which the SZA is changing. As a result of this measurement sequence, for every MLS SZA, there are typically two corresponding TMF measurements taken during the time period covering the MLS SZA. For example, if a MLS measurement occurred at a SZA at which FTUVS was taking the Nth west limb measurement, West(N), the TMF OH data out of two pairs of spectra, East(N-1)/West(N) and East(N)/West(N), were selected to compare with the MLS results. Only when the SZA fell in the FTUVS telescope adjustment between two limbs, was there exactly one pair of spectra and thus one TMF data to be selected. The corresponding TMF total OH abundance results during selected days are plotted in Figure 1 as well (blue solid points). In addition, to show the seasonal variation, TMF results around 21:06 UT during other days without comparable MLS data are also shown with the blue open points. The large gaps in the time series of MLS data are due to the MLS v2.2 reprocessing.

It is interesting that during days with high OH levels the TMF OH abundance is generally higher than the MLS column, leaving a positive residual in the lower atmosphere. During winter days with low OH, however, the partial OH column from MLS is often similar to or even higher than the TMF total OH column, resulting in a negligible or even negative residual in the lower atmosphere. A seasonal histogram of this residual clearly illustrates this trend (Figure 3). The highest OH residual occurs in summer ($4.3 \times 10^{12} - 8.8 \times 10^{12} \text{ cm}^{-2}$). The fall data set, with the majority of data in September, shows smaller OH residuals centered near $3 \times 10^{12} \text{ cm}^{-2}$. The spring data shows slightly lower OH residuals, while during winter the mean residual is below zero. A weaker seasonal variation in MLS OH measurements than TMF OH abundance is thus suggested. For example, the mean TMF OH column increases near 12% from $5.73 \times 10^{13} \text{ cm}^{-2}$ in March, 2005 to $6.40 \times 10^{12} \text{ cm}^{-2}$ in September, 2005, while the mean MLS OH column remains at the similar level in both months (< 2% increase from March to September).

3.2 The lower atmospheric residual estimated with GEOS-Chem

In order to make a total column comparison between MLS and TMF, the lower atmospheric OH partial column that is missing from MLS data has to be estimated. GEOS-Chem v5-07-08 outputs for 2003 monthly mean are used to determine this OH residual. The tropospheric part is directly calculated with GEOS-Chem [Bey et al, 2001][Bloss et al, 2005], while the lower stratosphere part is calculated with the Harvard 2-D model implemented in GEOS-Chem [Schneider et al, 2000]. In this model version, fifty five vertical layers are used to cover the entire atmosphere.

Figure 5 shows the GEOS-Chem 2003 monthly mean OH outputs extracted for TMF area. To integrate the OH densities into columns, the pressure data was converted into altitudes using scale heights derived from GEOS-Chem temperature fields. The partial OH column below 21.5 hPa for each month was then calculated. However, the average surface pressure in the $2^\circ \times 2.5^\circ$ model grid covering TMF area is ~ 950 hPa, different from the TMF surface pressure (~ 790 hPa) due to the higher elevation of TMF. TMF falls in the 5th model layer. While the exclusion of the lowest four layers most likely introduces an underestimation of the OH residual at TMF, the integration from the model surface gives an upper end of the estimation. Therefore, two partial OH columns were calculated, starting from the surface and the 5th model layer, as the maximum and the minimum estimations of the OH residual. The minimum is typically 8 – 12% smaller than the maximum, depending on the time of the year (Figure 7).

In order to convert the monthly mean OH residual into MLS overpass time data, a conversion factor has to be estimated for each month. Given the diurnal SZA variation in each month calculated with MICA, these conversion factors were derived based on observations and modeling of the variation of OH density with SZA in the upper troposphere and lower stratosphere [Salawitch et al, 1994][Wennberg et al, 1995]. The monthly mean OH residual around the satellite overpass time were thus calculated by applying these factors (Figure 7). The daily OH residual was obtained through a linear interpolation of the mean of the maximum and minimum estimations. A combined total OH column is thus obtained by adding the GEOS-Chem partial OH column to the MLS OH column (the red points in Figure 1).

To validate this semi-quantitative approach, a newer version of GEOS-Chem (v7-04-10) with hourly OH outputs was employed to generate overpass time OH for selected months. Since March and September, 2005 have the most concentrated MLS and TMF data, these months were selected. The major differences and similarities of the two model versions are listed in Table 1. The v7-04-10 model generates instantaneous OH profiles in the troposphere in every hour. The outputs at 21:00 UT are expected to be the closest to the results at MLS overpass time. The maximum tropospheric OH columns are calculated from the ground surface in the $2^{\circ} \times 2.5^{\circ}$ model grid covering TMF to the tropopause, while the minimum tropospheric columns are calculated from the TMF elevation to the tropopause. These columns are marked as the upper and lower error bars in Figure 9. The equivalent tropospheric OH columns on these days derived from v5-07-08 GEOS-Chem 2003 monthly mean results are plotted together for a comparison. The dotted green lines show a 30% uncertainty range of the estimated columns. Considering the differences of these two model versions, these results reach an acceptable agreement. In particular, in September, during 88% of the calculated days the 2005 model calculations for 21:00 UT fall in the $\pm 30\%$ range of the derived overpass time OH columns from the 2003 monthly mean. The fact that GEOS-Chem v7-04-10 results are generally higher than those from v5-07-08 is consistent with the previous comparisons of OH outputs from different versions of GEOS-Chem. [Wu et al, 2007] reported significantly higher OH from models with GEOS-4 meteorology than those with GEOS-3 due to a 14% difference in radiative impacts from clouds. [Hudman et al, 2007] also reported significantly higher OH from GEOS-4 model simulations than measurements from Intex-NA. Since this OH residual estimated by GEOS-Chem is less than 12% of the total OH column, a 30% uncertainty in the GEOS-Chem estimation would contribute less than 3.6% to the total OH column. The above-described derivation of the OH residual using GEOS-Chem 2003 monthly mean outputs should thus be adequate for the purpose of the total OH column validation.

As shown in Figure 1, the combined total OH columns from “MLS + GEOS-Chem” agree well with the TMF total column measurements during most high OH days. During winter and early spring, however, the former is often larger than the latter.

3.3 Comparison of GEOS-Chem OH results with 1-D photochemical model calculations and observations

The JPL 1-D HO_x photochemical model was also employed to derive the OH vertical profiles in the lower stratosphere and the troposphere to compare with the above-described GEOS-Chem results. The 1-D model is constrained by MLS measurements of H₂O, O₃, N₂O, CO, and temperature. It has been previously employed for validation of MLS HO_x measurements for September, 2004 and 2005 [Pickett et al., 2006, 2007][Canty et al., 2006]. More details about of the model and the included chemical kinetics are described in [Canty et al., 2006]. *(Tim will probably add a short description of the model and his calculations here)*

Figure 11 shows a seasonal comparison of model results. The daily mean results from the 1-D HO_x model on March 15th, June 15th, September 23rd, and December 23rd in 2004 are compared with the corresponding GEOS-Chem monthly mean results. The 1-D model results are a combination of model calculations and observations. The model calculates OH profiles above 12 km altitude. The OH below 12 km is derived based on the STRAT (Stratospheric Tracers of Atmospheric Transport) observations on NASA ER-2 in the free troposphere [Wennberg et al., 1998]. Considering the variation of OH from the free troposphere to the boundary layer, observations from Meteorological Observatory Hohenpeissenberg in Germany [Rohrer and Berresheim, 2006] and Intex-NA (Intercontinental chemical Transport Experiment – North America) (see <http://www.espo.nasa.gov/intex-na/data.html> for details) are also used to derive the boundary layer OH. The agreement between GEOS-Chem and the 1-D HO_x model results is good in winter and spring. Small differences occur at 100 – 300 hPa where OH has the lowest density. For summer and fall, larger differences occur at the free troposphere, while the agreements above 12 km and in the boundary layer are generally good.

MLS measurements in the lower stratosphere are also shown in Figure 11. As mentioned earlier, the precision of MLS OH measurements below 21.5 hPa is poor. Nevertheless, the zonal mean OH data can be used to compare with the model calculations in the lower stratosphere, in particular below 21.5 hPa. For an easy comparison, the MLS data were converted into daily mean by applying the conversion factor described in section 3.2. Both model results agree with MLS within the measurement precision, except for June 15th, 2004 during which the MLS measurements are higher than both model results.

On September 23rd, 2004, measurements in the lower stratosphere from BOH and FIRS-2 close to the MLS overpass time are also compared with the model calculations (Figure 11). Details of the balloon flight on this day were given in [Pickett et al., 2006]. These observations agree with both model calculations.

At 100 – 200 hPa where the model results show small discrepancies, measurements from STRAT [Wennberg et al., 1998] at comparable latitudes (35.9 – 37.3°N for flight 960202, 37.9 – 40.5°N for flight 951031, 21.6 – 22.1°N for flight 951107) and longitudes (121.4 – 122.3°W for flight 960202, 122.2 – 122.9°W for flight 951031, 159.4 – 160.6 °W for flight 951107) are also converted into daily mean OH to compare with GEOS-Chem monthly mean results (Figure 13). The STRAT observations agree well with the GEOS-Chem data.

4. Discussions

4.1 Linear correlation of the total OH columns

Figure 15 shows the linear correlation of the total OH columns from “MLS + GEOS-Chem” and from TMF during September, 2004 – April, 2007. The data points are color-coded. Black indicates that TMF measurements occurred on the same day as MLS measurements. Red means that the measurements were one day apart. It should also be noted that some TMF data points are used more than once in this correlation analysis. For example, TMF data on 9/24/2004 is compared with the MLS data on 9/24/2004 as a same-day data point and also compared with MLS data on 9/25/2004 as a next-day data point. The horizontal error bars are the spectral fit uncertainties from the TMF data analysis. The vertical error bars are the RSS (root sum square) of MLS spectral retrieval uncertainties and an assumed 30% uncertainty in the estimation of the GEOS-Chem partial OH columns. A number of different least-squares linear regression methods were applied to the data in Figure 15 to get a complete view of the correlation. The results are listed in Table 3.

1. **Standard linear regression.** Without considering the errors, the linear fit through zero generates a slope of 1.065, which indicates a remarkable agreement, within 6.5%, between these two groups of total OH columns. When the slope is constrained to unity, the linear fit results in an intercept of $0.397 \times 10^{13} \text{ cm}^{-2}$. Considering the range of the TMF total OH columns in this study ($\sim 3.8 \times 10^{13} - 7.1 \times 10^{13} \text{ cm}^{-2}$), this intercept implies a rather small offset of about 5.6 – 10 %, depending on the time of the year. The correlation coefficient R is as good as 0.854. A standard linear fit without constraints, however, gives a much smaller slope (0.673) and a much larger intercept ($2.203 \times 10^{13} \text{ cm}^{-2}$). A closer look at the correlation in Figure 15 suggests a good agreement at high OH but a difference at low OH conditions (also shown in Figure 1), which significantly influences the linear fit results. The standard fit with y error bars (uncertainties in the “MLS + GEOS-Chem” total OH column) weighted show very similar results. It has to be noted that the above-mentioned least-squares linear regression calculations all assume that x (TMF OH column) is the reference with no error. It is then worth to investigate the linear regression results considering deviations and errors in both x and y directions.
2. **Contour mapping of the orthogonal Chi square.** An orthogonal least square regression takes into account the deviation from the fitted line to the measured points in both x and y directions (Figure 17). Instead of minimizing the sum of the squared vertical distance from the measured data to the fitted line as in a standard linear fit, the orthogonal regression (or “total” least-squares regression) finds the minimum of the sum of the squared perpendicular distance between the measurements (x, y) and the predictions (X, Y). (see equation (1)).

$$\chi^2_{reduced} = \frac{1}{N-2} \cdot \sum_{i=1}^N [(X_i - x_i)^2 + (Y_i - y_i)^2] = \frac{1}{N-2} \cdot \sum_{i=1}^N \left[\frac{(x'_i - x_i)^2 (y'_i - y_i)^2}{(x'_i - x_i)^2 + (y'_i - y_i)^2} \right] \quad (1)$$

Here, $y'_i = a + bx_i$ and $x'_i = (y_i - a)/b$. N is the total number of points and N – 2 is the degree of freedom. Since the errors are not weighted, the reduced chi squared $\chi^2_{reduced}$ calculated in (1) is not in the same order of magnitude as unity. Nevertheless, the contour mapping of $\chi^2_{reduced}$ is a useful approach to illustrate

the distribution of the minima of $\chi^2_{reduced}$ with the variation of both intercept a and slope b . As shown in Figure 17, the shape of the contours is far from circular. The long and narrow contours are diagonal, going from slopes near unity and intercepts close to zero (shown by the red solid lines) down to smaller slopes and larger intercepts. The green cross shows the best orthogonal fit without error weighting at a slope of 0.76 and an intercept of $1.725 \times 10^{13} \text{ cm}^{-2}$.

3. **Orthogonal least-squares linear fit with both x and y errors weighted.** The orthogonal linear fit with both x and y errors (σ_x and σ_y) weighted finds the minimum χ^2 as shown in equation (2),

$$\chi^2 = \sum_i \left[\frac{(X_i - x_i)^2}{\sigma_{xi}^2} + \frac{(Y_i - y_i)^2}{\sigma_{yi}^2} \right] \quad (2)$$

The optimal a and b are found by solving equation (2), which is further rewritten as equation (3), and equation (4) [Reed 1988, 1991][York, 1966][Press et al, 1992].

$$\chi^2 = \sum_i \frac{(y_i - a - bx_i)^2}{\sigma_{yi}^2 + b^2 \sigma_{xi}^2} \quad (3)$$

$$a = \frac{\sum_i \frac{y_i - bx_i}{\sigma_{yi}^2 + b^2 \sigma_{xi}^2}}{\sum_i \frac{1}{\sigma_{yi}^2 + b^2 \sigma_{xi}^2}} \quad (4)$$

The results of this orthogonal linear fit are shown in both Table 3 and Figure 15 (the green line). The slope is found to be 0.835 with an intercept of $1.308 \times 10^{13} \text{ cm}^{-2}$. This confirms the trend shown by the standard linear regression and the contour mapping of orthogonal chi squares, although the inclusion of both error bars significantly improves the slope and the intercept. A weaker seasonal variation in MLS measurements than TMF measurements and a possible offset between these results are thus suggested.

It has to be noted that another method different from the SZA method described in section 3.1 was also employed to select the comparable TMF data at MLS overpass time

for this correlation investigation. Instead of selecting two data points (on most days) measured during time spans covering the MLS SZA, this alternative method applies a second order polynomial (parabolic function) fit to the diurnal variation of TMF OH data during each day. The TMF OH column result at the MLS overpass time was derived from the fitted curve. This “parabolic selection” gives linear correlation results between “MLS + GEOS-Chem” and TMF total OH columns very similar to, but not better than, those shown in Figure 15 and Table 3.

4.2 Seasonal and SZA variations of the total OH columns

Since the correlation analysis show different seasonal variations in both measurements, it is necessary to investigate the correlation in each season. Figure 19 shows the seasonal histograms of the total OH columns from “MLS + GEOS-Chem” and TMF. The distribution of these two groups of total OH columns shows a good correlation in summer though the dataset is small. During spring and fall, the datasets are reasonably large. Their distributions generally agree, with TMF results being slightly lower. During winter, however, there is a significant shift between these two measurements.

The histograms at different SZA bins (Figure 21) help to further investigate the difference in seasonal variations. The data with SZAs of $[20^\circ, 30^\circ]$ are corresponding to the summer time data in Figure 19. The SZA bin of $[30^\circ, 40^\circ]$ has a reasonably large dataset and shows a good agreement between the total OH columns. When the SZA is above 40° , a noticeable shift occurs. At $[50^\circ, 60^\circ]$, the combined total OH column from MLS + GEOS-Chem is considerably larger than TMF measurements. The two-group independent T test results are also summarized in Table 5, which provides quantitative insights to the seasonal comparison. The mean of the TMF total OH columns decreases from the $6.885 \times 10^{13} \text{ cm}^{-2}$ at the smallest SZAs to the $4.756 \times 10^{13} \text{ cm}^{-2}$ at the largest SZAs, while the difference of means (DOM) increases significantly from 1.02×10^{12} to $4.99 \times 10^{12} \text{ cm}^{-2}$. Though the dataset at SZA of $[20^\circ, 30^\circ]$ is likely too small, the data at the $[30^\circ, 40^\circ]$ bin shows a good agreement between TMF and “MLS + GEOS-Chem”. The mean of the combined total columns in this bin is only 3% larger than the mean of TMF total columns. At the largest SZA bin, the former is shown to be 10.5% larger than the latter. The T value also increases from 1.12 to 5.86 with the increase of SZA from $[20^\circ, 30^\circ]$ to $[50^\circ, 60^\circ]$. At a 95% confidence level, the data at SZAs above 40° show statistically significant

differences, especially at 50° and above. At large SZAs in winter, the view angle of the FTUVS instrument is toward the south. The larger the SZA is, the further the observed air mass deviates from TMF. For 45 km and 75 km altitudes where OH density often peaks, the horizontal deviation for a SZA of 60° is about 78 km and 130 km. While this change in instrument viewing angles may be a source of the differences in the observations, it is rather small, especially considering the size of the latitude grid of MLS results.

Figure 23 shows the decay of the total OH columns with the increase of SZA for both “MLS + GEOS-Chem” and TMF. The SZA variation or seasonal variation of MLS results is clearly weaker than TMF measurements. Since MLS and the FTUVS measures OH at the microwave and the UV region, respectively, the uncertainties in the relative cross sections from microwave to UV could contribute significantly to the different seasonal variations in these measurements, which may explain the slope of the linear correlation in Figure 15.

While the estimation of the OH residual may also contribute to the differences in these OH total columns in both slope and the intercept errors, the impact should be small considering the fact that this OH residual counts for less than 12% of the total OH abundance. The intercept of $1.308 \times 10^{13} \text{ cm}^{-2}$ (Table 3) implies a possible offset, which is larger than twice of the magnitude of the maximum OH residual. The majority of the discrepancy should thus come from one of the measurements or both. The MLS measures OH at both daytime and nighttime. The nighttime data are used to correct the daytime measurements, which minimizes the possible offset. While the FTUVS measures OH only during the day, the measurement technique is straightforward and does not involve any major source of offset. Since our synthetic Doppler OH line shape used in the spectral fit is modeled for 250 K, the average OH column temperature based on a OH density weighted model of the atmospheric temperature profile [Cageao et al, 2001], the pressure broadening in the lower atmosphere could in principle influence the line shape and contribute errors to the retrieval results. However, the OH abundance in the lower atmosphere where pressure broadening is significant is small. Thus the potential impact is less than a few percent. Further investigations are required to understand the differences in these observations. Nevertheless, considering the large discrepancies of 10 – 65% in

the previous OH column measurements at various sites in the mid-latitudes with various instruments [Mills et al, 2002][Iwagami et al, 1998], the agreement between TMF and MLS measurements over a period of near 3 years is remarkable.

5. Conclusions

The MLS OH measurements at mid-latitude are validated with the FTUVS measurements of total OH abundance at TMF from 2004 to 2007. This is the first seasonal and inter-annual comparison of OH measurements from space and the ground-level. To compare the total OH column results, the OH residual in the lower atmosphere where MLS measurements are missing is estimated using GEOS-Chem. In general, the total OH columns from MLS + GEOS-Chem and TMF agree, especially during high OH seasons (small SZAs). A linear correlation through zero shows a remarkable agreement within 6.5%.

Detailed statistical investigations, however, show certain disagreements during low OH seasons (large SZAs), which suggests a weaker seasonal variation in MLS measurements than TMF measurements and a possible offset. Since MLS and FTUVS measures OH at very different spectral regions, it is speculated that the difference in the relative absorption cross section from UV to microwave may contribute to the observed difference in seasonal variations or the slope error in the linear correlation. Other possible sources of discrepancies include, but are not limited to, the estimation of the OH residual and the different instrument viewing angles at large SZAs. In addition, the summer time data are too sparse, which may bias the linear fit. More data during summer will be available as the MLS reprocessing goes. Further investigations with more complete datasets are required to understand the differences between these measurements.

Acknowledgement

References

[To be updated]

Bey, I. et al., *Global modeling of tropospheric chemistry with assimilated meteorology: Model description and evaluation*, *J. Geophys. Res.*, 106(D19), 23,073 – 23,096, 2001

Bloss, W.J., M.J. Evans, J.D. Lee, R. Sommariva, et al, *The oxidative capacity of the troposphere: coupling of field measurements of OH and a global chemistry transport model*. *Faraday Discuss.*, 130, 425-436, 2005

Benkovitz, C. M., et al., *Global gridded inventories of anthropogenic emissions for sulfur and nitrogen*, *J. Geophys. Res.*, 101 (D22), 29,239 – 29,253, 1996

Cageao, R.P., J.F. Blavier, J.P. McGuire, et al., *High-resolution Fourier-transform ultraviolet-visible spectrometer for the measurement of atmospheric trace species: Application to OH*, *Appl. Opt.*, 40, 2024 – 2030, 2001

Canty, T., H.M. Pickett, R.J. Salawitch, et al., *Stratospheric and mesospheric HOx: results from Aura MLS and FIRS-2*. *Geophys. Res. Lett.* 33, L12802, doi:10.1029, 2006

Cheung, R., K.F. Li, S. Wang, et al., *An improved method for retrieving hydroxyl radical (OH) abundances from ultraviolet spectra*, to be submitted to *Appl. Opt.*, 2007

Froidevaux et al, 2006

Duncan, B. N. et al., *Interannual and seasonal variability of biomass burning emissions constrained by satellite observations*, *J. Geophys. Res.*, 108(D2), 4100, doi:10.1029/2002JD002378, 2003

Li, K.F., R.P. Cageao, E.M. Karpilovsky, et al., *OH column abundance over Table Mountain Facility, California: AM-PM diurnal asymmetry*, *Geophys. Res. Lett.*, 32, L13813, 2005

Iwagami et al, 1998

Mills, F.P, R.P. Cageao, V. Nemtchinov, et al., *OH column abundance over Table Mountain Facility, California: Annual average 1997 – 2000*, *Geophys. Res. Lett.*, 29(25), 1742, 2002

Mills, F.P., R.P. Cagiao, S.P. Sander, et al., OH column abundance over Table Mountain Facility, California: Intraannual variations and comparisons to model predictions for 1997 – 2001, *J. Geophys. Res.*, 108(D24), 4785, 2003

Muller et al, 1999

Olivier, J.G.J. and J.J.M. Berdowski, Global emissions sources and sinks. In: Berdowski, J., Guicherit, R. and B.J. Heij (eds.) "The Climate System", pp. 33-78. A.A. Balkema Publishers/Swets & Zeitlinger Publishers, Lisse, The Netherlands. ISBN 90 5809 255 0, 2001

Osterman, G.B. et al. Balloon-borne measurements of stratospheric radicals and their precursors: Implications for the production and loss of ozone, *Geophys Res. Lett.*, 24, L1107-L1110, 2005

Pickett, H.M., B.J. Drouin, T. Canty, et al., Validation of Aura MLS HOx measurements with remote-sensing balloon instruments, *Geophys. Res. Lett.*, 33, L01808, 2006

Pickett, H.M., Microwave Limb Sounder THz module on Aura, *IEEE Trans. Geosci. Remote Sens.*, 40(5), 1122 – 1130, 2006

Pickett, H.M., B.J. Drouin, T. Canty, et al., Validation of Aura Microwave Limb Sounder OH and HO₂ measurements, Submitting to *J. Geophys. Res.*, 2007

Press, W.H., et al, *Numerical Recipes (The art of scientific computing)* 1992

Reed, B.C., Linear least-squares fits with errors in both coordinates, *Am. J. Phys.* 57(7), 642 – 646, 1988

Reed, B.C., least-squares fits with errors in both coordinates. II: Comments on parameter variances, *am. J. Phys.* 60(1), 59 – 62, 1991

Rohrer, F. and H. Berresheim, Strong correlation between levels of tropospheric hydroxyl radicals and solar ultraviolet radiation. *Nature*, 442, doi:10.1038, 2006

Salawitch, R.J., S.C. Wofsy, P.O. Wennberg, et al., The diurnal variation of hydrogen, nitrogen, and chlorine radicals: implications for the heterogeneous production of HNO₂, *Geophys. Res. Lett.*, 21(23), 2551 – 2554, 1994

Salawitch, R.J., et al., Sensitivity of ozone to bromine in the lower stratosphere, Geophys. Res. Lett., 32, L05811, 2005

Schneider et al, 2000

Waters, J.W., L. Froidevaux, R.S. Harwood, et al., The Earth Observing System Microwave Limb Sounder (EOS MLS) on the Aura satellite, IEEE Trans. Geosci. Remote Sens., 40(5), 1075 – 1092, 2006

Wennberg et al, 1995

Wennberg, P.O., T.F. Hanisco, L. Jaegle, et al., Hydrogen radicals, nitrogen radicals, and the production of O₃ in the upper troposphere, Science, 279(49), doi:10.1126, 1998

York, D., Least-squares fitting of a straight line, Canadian Journal of Physics, 44, 1079 – 1086, 1966

Tables

	2003 Monthly Mean	2005 Hourly Outputs
Model Version	V5-07-08	V7-04-10
Meteorology	GEOS-3 meteorological Data in 2001	Current GEOS-4 meteorology
Horizontal Resolution	Results were re-gridded into GEOS-4 resolution (2 X 2.5)	GEOS-4 resolution (2 X 2.5)
Vertical Resolution	55 layers	30 layers
Emissions	The major emissions (fossil fuel, biomass burning etc.) are the same	

Table 1. Side-by-side comparison of the two versions of GEOS-Chem used in this study

Type of Linear Fit		Slope	Intercept (10^{13}cm^{-2})	R
No error weighted	Fit through 0 	1.065±0.005	0	0.854
	Fit with unity slope 	1	0.397±0.027	0.854
	Standard fit 	0.673±0.029	2.203±0.161	0.854
Standard fit with y errors weighted 		0.686±0.019	2.095±0.101	0.850
Orthogonal fit with x and y error s weighted 		0.835±0.185	1.308±0.003	0.855

Table 3. The results of the linear correlation between the sum of MLS and GEOS-Chem partial OH columns and the TMF total OH columns (see Figure 15)

	SZA [20°, 30°]		SZA [30°, 40°]		SZA [40°, 50°]		SZA [50°, 60°]	
Sample	MLS + GEOS- Chem	TMF						
Mean (10^{13}cm^{-2})	6.987	6.885	6.353	6.169	6.085	5.702	5.256	4.756
T value	1.12		2.09		4.36		5.86	
Degree of freedom (DOF)	8		55		71		69	
Difference of Means (DOM) (10^{13}cm^{-2})	0.102		0.184		0.384		0.499	

Table 5. The two-sample independent T-test results for the total OH columns from TMF and MLS+GEOS-Chem for different SZAs (see Figure 10 for the corresponding histogram plots)

Figures

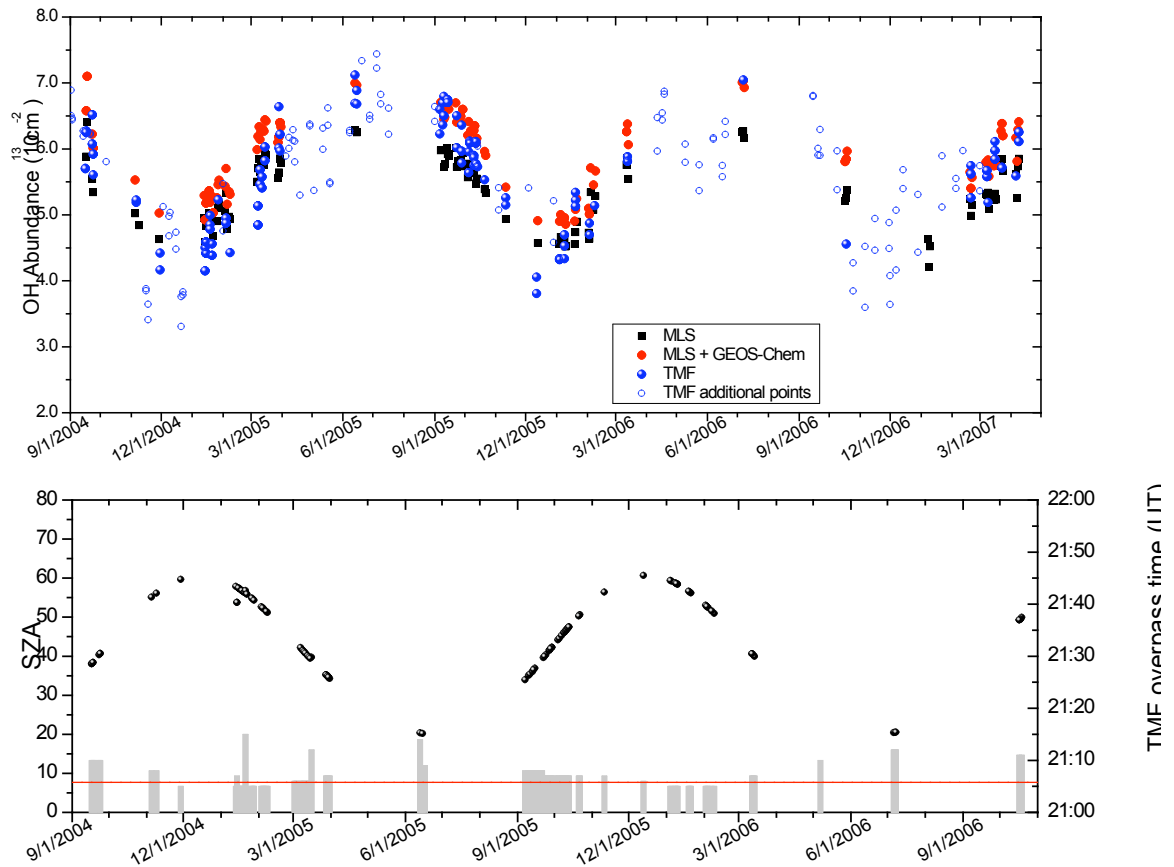


Figure 1. OH column results from MLS, MLS + GEOS-Chem, and TMF

Black squares indicate integrated MLS OH column results for altitudes with pressure lower than 21.5 hPa with the corresponding error bars. The total OH column from the sum of MLS and GEOS-Chem partial OH columns are shown in red circles. Blue circles are the TMF OH abundance. The days selected for a close comparison are indicated with solid circles, while the open circles show the additional data for a general seasonal variation. The SZA of MLS measurements is plotted in the lower panel. The corresponding overpass time at TMF area is plotted as gray vertical bars in the same panel. The average overpass time is about 21:06 UT, marked with the red horizontal line.

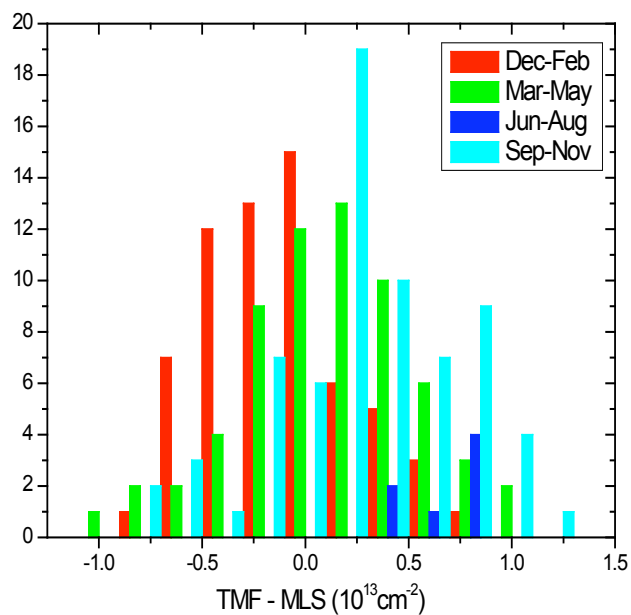


Figure 3. Histogram of the residual OH in the lower atmosphere (below 21.5 hPa) calculated by TMF total OH column minus MLS partial OH column

The selected days during 2004 – 2007 are grouped into four seasons. The vertical bars show the frequency of the occurrence of the corresponding residual OH during the specific season.

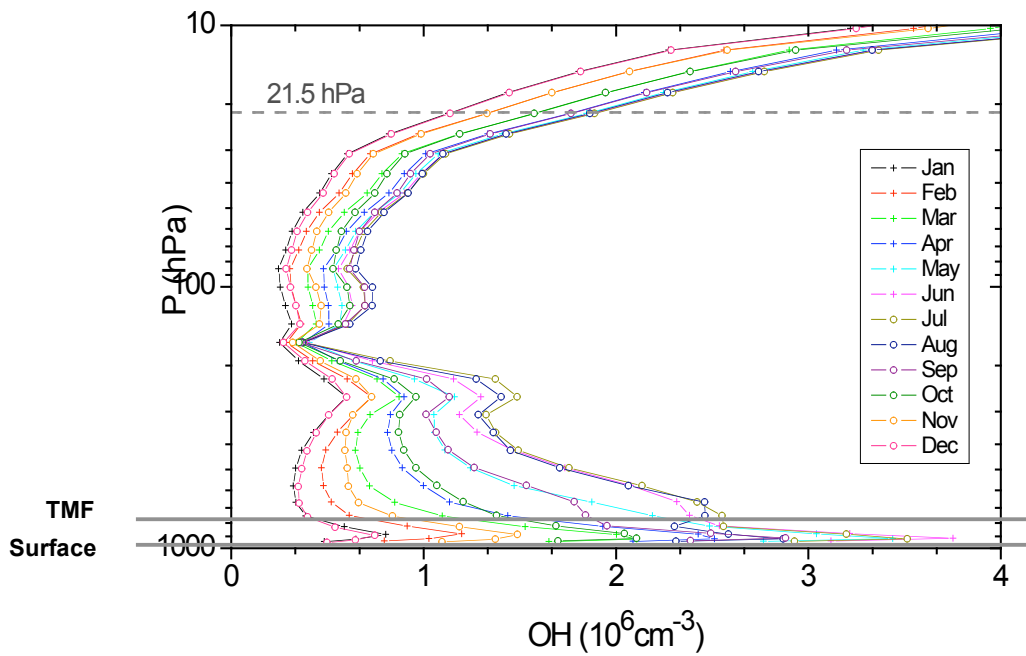


Figure 5. Monthly mean OH vertical profiles in 2003 calculated with GEOS-Chem

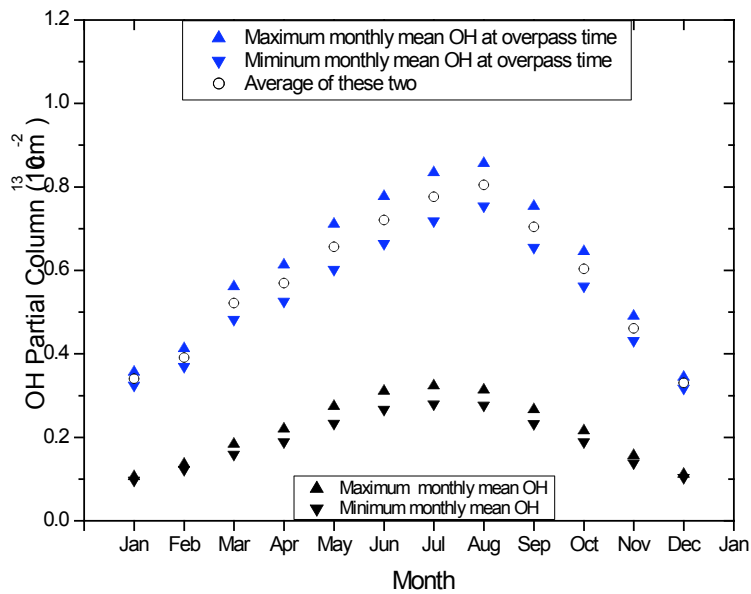


Figure 7. GEOS-Chem monthly mean OH partial columns before and after applying conversion factors

The black points are the monthly mean values over 24hr and the blue points are the monthly mean results for satellite overpass time at TMF area. The upward triangles show the maximum

OH residual integrated from model surface to 21.5 hPa. The downward triangles show the minimum OH partial columns integrated from TMF to 21.5 hPa. The open circles are the mean of the upward and downward blue triangles. The linear interpolation of these open circles gives the daily OH residual missing from MLS measurements.

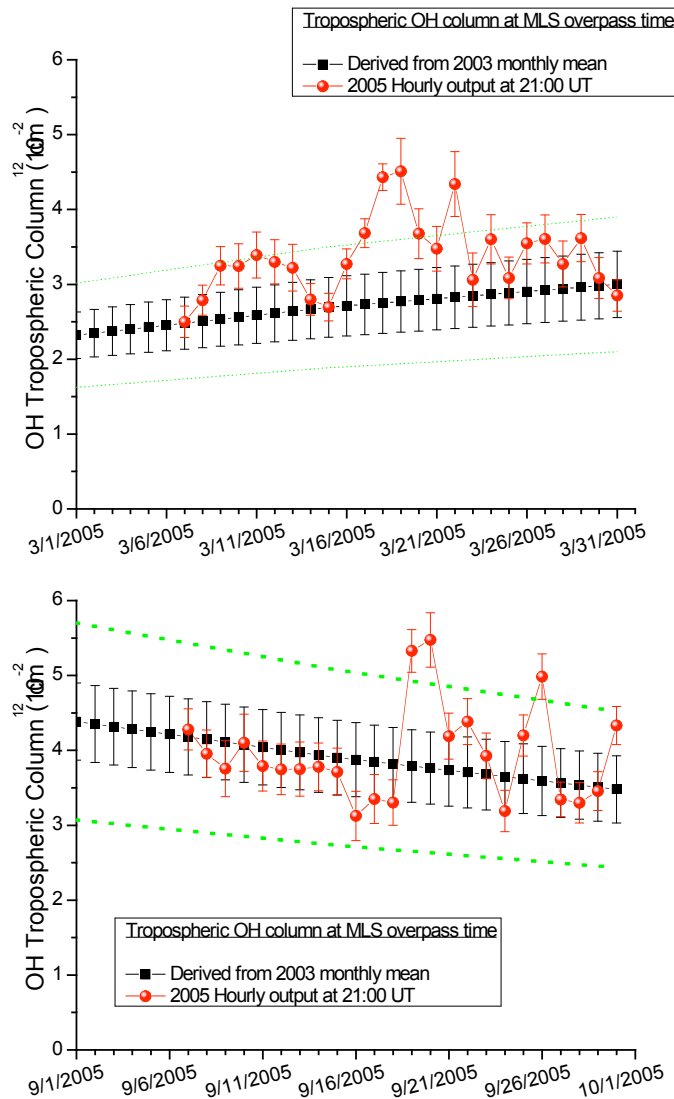


Figure 9. Comparison of the OH tropospheric columns at MLS overpass time from two versions of GEOS-Chem in March and September, 2005

Black indicates the tropospheric columns at MLS overpass time estimated from 2003 monthly mean results (v5-07-08). Red shows v7-04-10 outputs at 21:00 UT. The upper and lower error bars show the maximum and minimum estimations of the tropospheric OH column calculated from the model surface and TMF elevation, respectively, to the tropopause. The points are the mean of the maxima

and the minima. The $\pm 30\%$ uncertainty range of the derived tropospheric columns is marked with the green dotted lines.

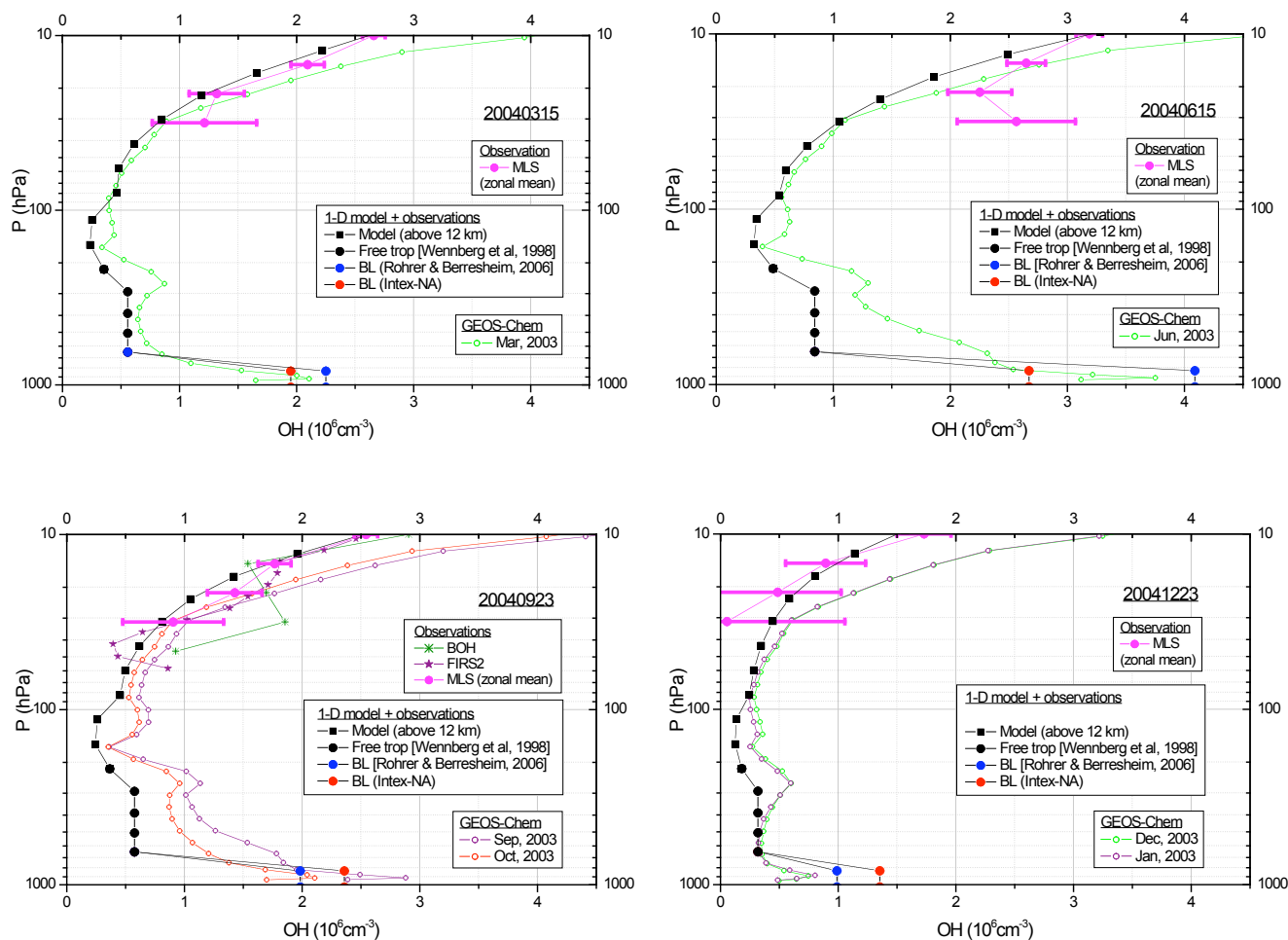


Figure 11. Comparison between field observations and model calculations of the OH distribution in the troposphere and lower stratosphere on a selected day for each season

The OH vertical profiles from the 1-D HO_x model are a combination of model calculations and observations. The model calculates daily mean OH vertical profiles above 12 km over TMF. The OH from 12 km to the boundary layer top is derived from the STRAT observations in the free troposphere. The boundary layer OH is derived from 2 sets of observations ([Rohrer and Berresheim, 2006] and Intex-NA). GEOS-Chem 2003 monthly mean OH profiles during the comparable months are shown. MLS measurements in the lower stratosphere and BOH and FIRS-2 measurements close to the MLS overpass time are converted into daily mean OH for an easy comparison.

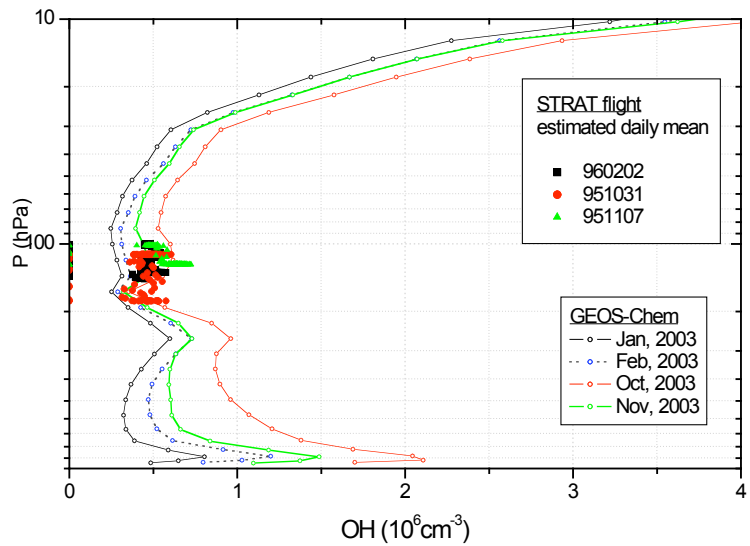


Figure 13. Comparison of OH distribution at 100 – 200 hPa from GEOS-Chem 2003 monthly mean outputs and STRAT observations in 1995 – 1996

The STRAT OH densities around the MLS overpass time (13:00 – 13:30 LST) on three selected days were converted into daily mean to compare with the GEOS-Chem monthly mean OH vertical profiles.

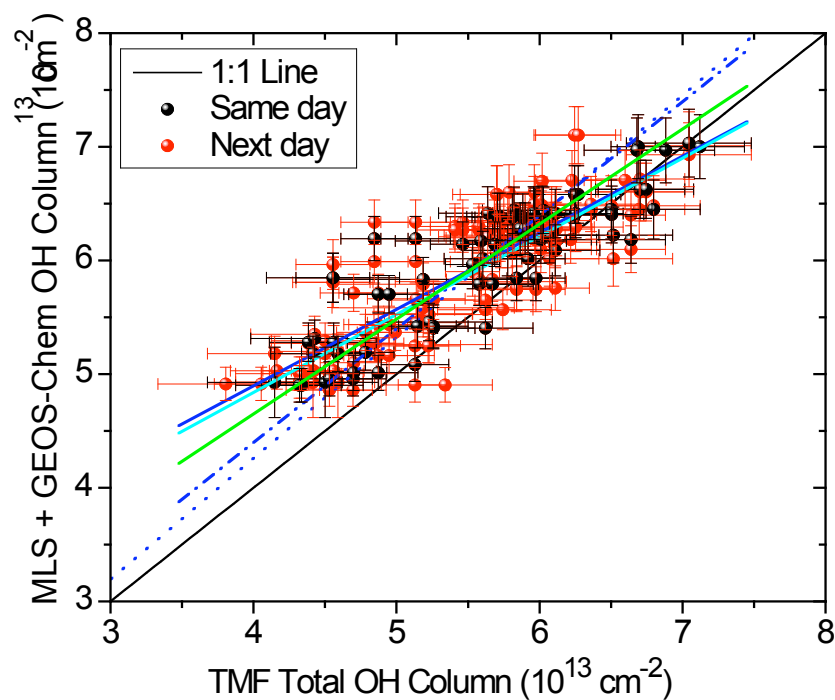


Figure 15. Correlation of OH Total Columns from TMF and MLS + GEOS-Chem

Data during days when MLS and TMF measurements were both available are indicated with black (“Same day” points). When MLS and TMF measurements are one day apart, the data are marked as “Next day” points in red. The horizontal error bars represent the spectral fit uncertainties of TMF measurements. The vertical error bars are the combination of MLS spectral retrieval uncertainties and an assumed 30% uncertainty in the partial OH column below 21.5 hPa estimated with GEOS-Chem 2003 monthly mean outputs. The legend of the fitted lines and the corresponding values of the slope and the intercept are shown in Table 3

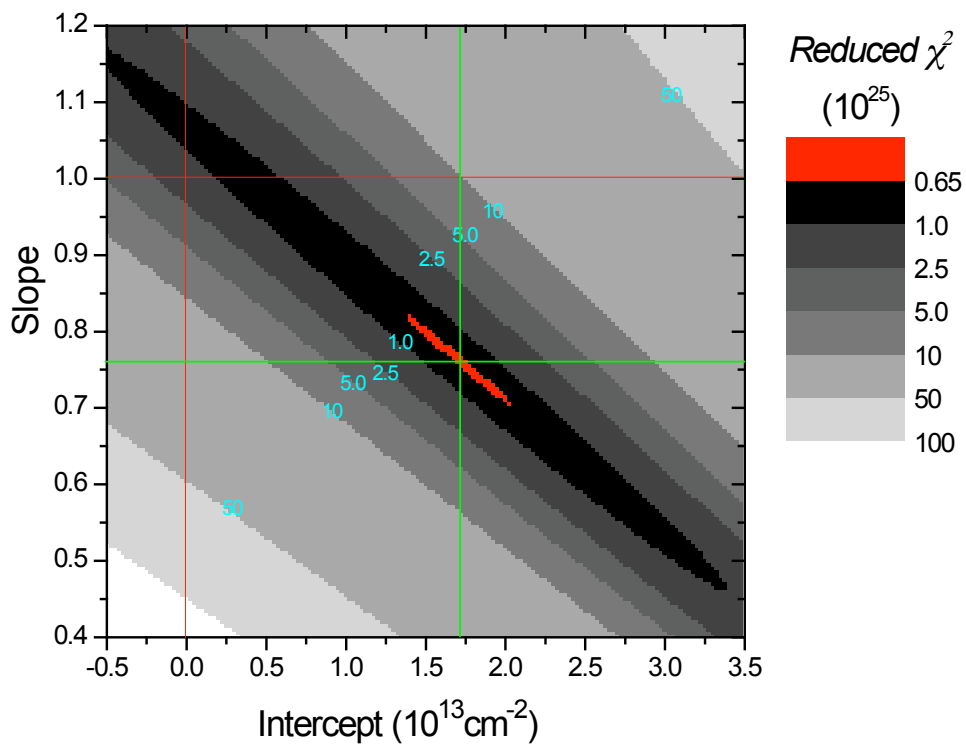
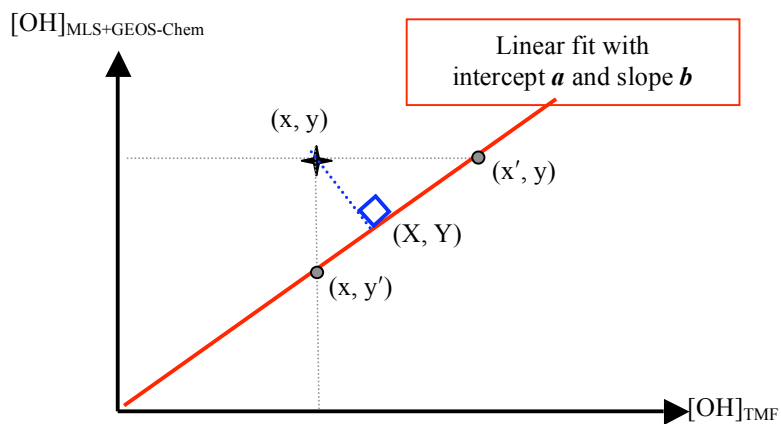


Figure 17. Contour mapping of the orthogonal Chi square calculations for the linear correlation between TMF total OH columns and the sum of MLS and GEOS-Chem partial OH columns shown in Figure 8

The top panel shows the schematics of the calculation of the “Orthogonal Chi Square”. The lower panel is the contour mapping of the reduced orthogonal Chi square with the change of the slope and the intercept. The calculation is given in equation (1). The red horizontal and vertical lines show the position of the linear regression with fixed slope (unity) and fixed intercept (zero), respectively.

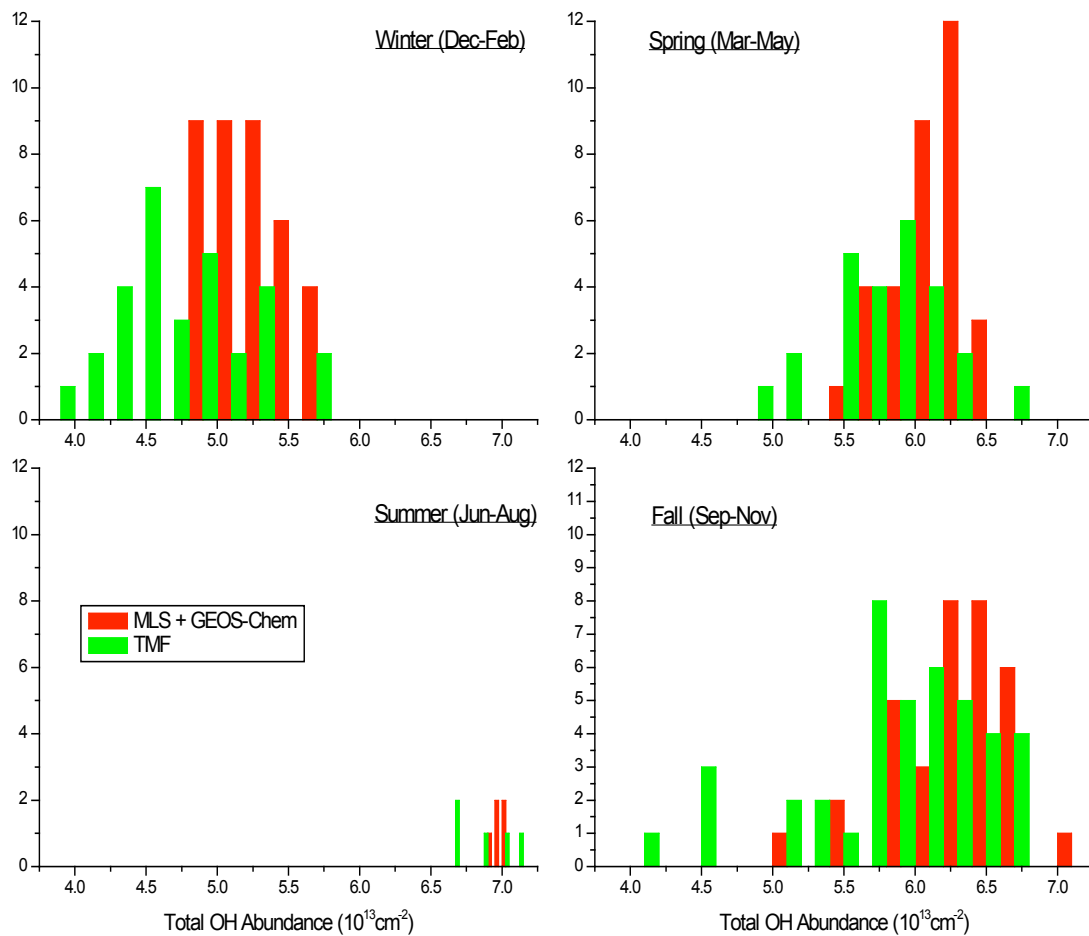


Figure 19. Seasonal histograms of total OH columns at satellite overpass time from TMF measurements and the sum of MLS and GEOS-Chem partial OH columns

The agreement is good in summer though the sample size is small. The fall and winter agreements are fairly good as well. In winter the OH columns from MLS + GEOS-Chem are significantly higher than TMF.

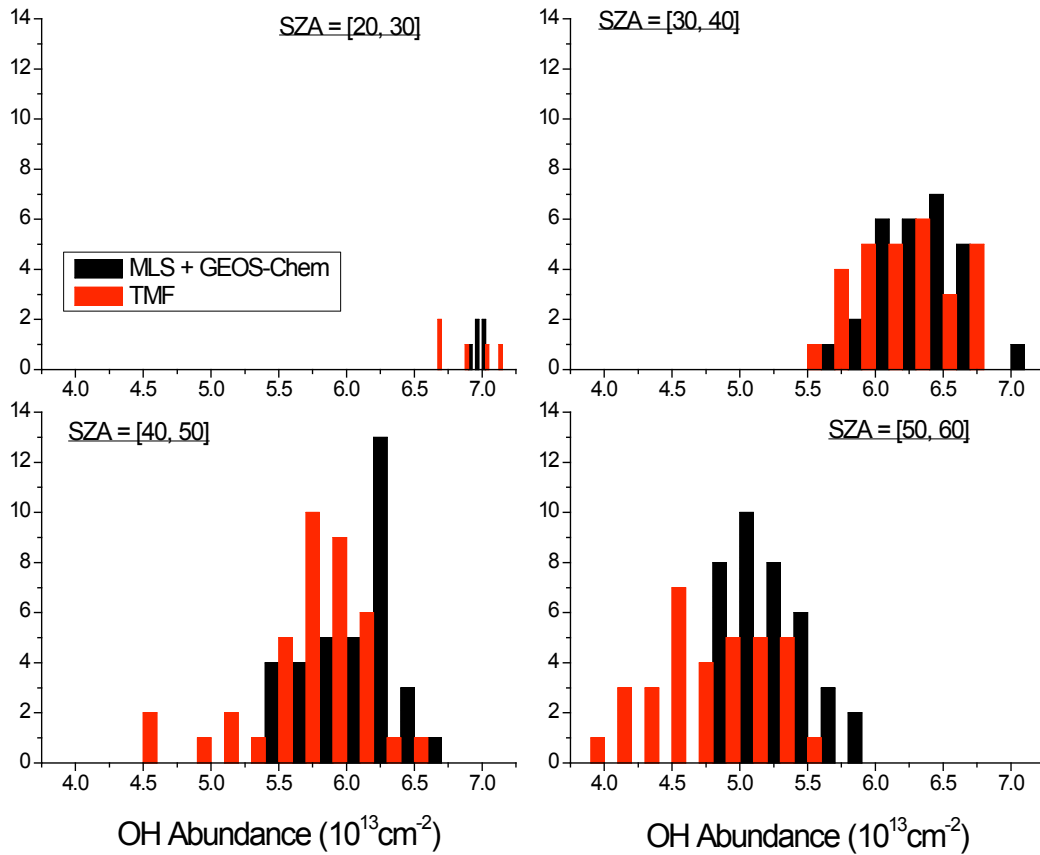


Figure 21. Histograms of total OH columns from TMF measurements and the sum of MLS and GEOS-Chem partial OH columns for different SZA ranges

Data with SZA below 40° show a good agreement between MLS + GEOS-Chem and TMF measurements. Above 40° SZA differences between the measurements are observed, especially for the SZA bin of [50, 60]. The corresponding two-sample independent T-test results for each SZA bin, including T values, the degree of freedom (DOF) and the difference of mean (DOM), are listed in Table 3.

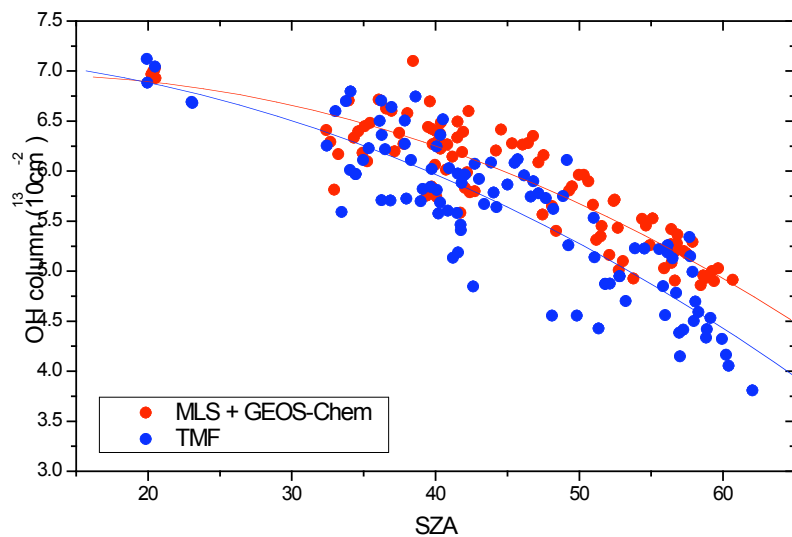


Figure 23. Comparison of SZA variations of the total OH columns from “MLS + GEOS-Chem” and TMF

The red and blue curves are second order fits of the decay of “MLS + GEOS-Chem” and TMF total columns with the increase of SZA